AD-A165 237 TARGET PARAMETER ESTIMATION IN THE NEAR-FIELD WITH TWO SENSORS(U) CONNECTICUT UNIV STORRS DEPT OF ELECTRICAL ENGINEERING AND CO.. H SHERTUKDE ET AL. JAN 86 TR-86-2 1/1

UNCLASSIFIED N00014-84-K-0492 F/G 17/7 NL

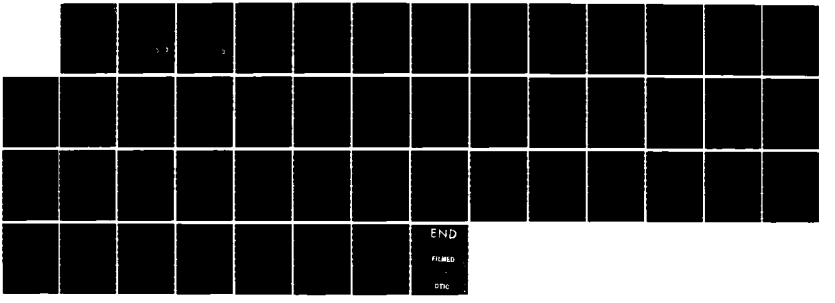

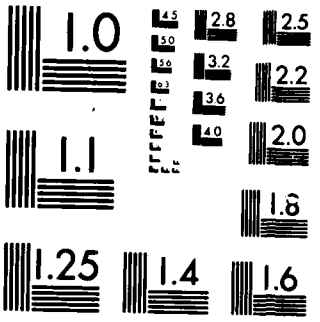

(12)

The University of Connecticut

SCHOOL OF ENGINEERING

Storrs, Connecticut 06268

Target Parameter Estimation in the Near-Field with Two Sensors

H. Shertukde

and

Y. Bar-Shalom

Technical Report TR-86-2

January 1986

Department of

Electrical Engineering and Computer Science

Target Parameter Estimation in the Near-Field with Two Sensors

H. Shertukde
and
Y. Bar-Shalom

Technical Report TR-86-2

January 1986

SECURITY CLASSIFICATION OF THIS PAGE *(When Data Entered)*

REPORT DOCUMENTATION PAGE

READ INSTRUCTIONS BEFORE COMPLETING FORM

1. REPORT NUMBER: TR-86-2	2. GOVT ACCESSION NO.
3. RECIPIENT'S CATALOG NUMBER	
4. TITLE *(and Subtitle)*: Target Parameter Estimation in the Near-Field with Two Sensors	5. TYPE OF REPORT & PERIOD COVERED: Annual 1984-85
	6. PERFORMING ORG. REPORT NUMBER
7. AUTHOR(s): H. Shertukde & Y. Bar-Shalom	8. CONTRACT OR GRANT NUMBER(s): N00014-84-K-049-2
9. PERFORMING ORGANIZATION NAME AND ADDRESS: Univ. of Conn., U-157 Storrs, CT 06268	10. PROGRAM ELEMENT, PROJECT, TASK AREA & WORK UNIT NUMBERS
11. CONTROLLING OFFICE NAME AND ADDRESS	12. REPORT DATE: Jan. 1986
	13. NUMBER OF PAGES: 46
14. MONITORING AGENCY NAME & ADDRESS *(if different from Controlling Office)*: ONR Code 411 Arlington, VA 22217	15. SECURITY CLASS. *(of this report)*: Unclassified
	15a. DECLASSIFICATION/DOWNGRADING SCHEDULE

16. DISTRIBUTION STATEMENT *(of this Report)*

Unlimited

DISTRIBUTION STATEMENT A
Approved for public release
Distribution Unlimited

17. DISTRIBUTION STATEMENT *(of the abstract entered in Block 20, if different from Report)*

18. SUPPLEMENTARY NOTES

19. KEY WORDS *(Continue on reverse side if necessary and identify by block number)*

Sonar, Passive Tracking, Distributed Field of Sensors

20. ABSTRACT *(Continue on reverse side if necessary and identify by block number)*

DD FORM 1 JAN 73 1473 EDITION OF 1 NOV 65 IS OBSOLETE
S/N 0102-LF-014-6601

Unclassified
SECURITY CLASSIFICATION OF THIS PAGE *(When Data Entered)*

TARGET PARAMETER ESTIMATION IN THE NEAR-FIELD WITH TWO SENSORS

HEMCHANDRA M. SHERTUKDE and YAAKOV BAR-SHALOM

Electrical Engineering and Computer Science Department,

University of Connecticut, U-157,

Storrs, CT 06268

ABSTRACT

A performance prediction procedure is developed for the evaluation of a passive tracking technique for the localization of targets in the near-field of the sensors. The target moves in a three-dimensional space with a constant velocity at a constant depth. The parameter vector is thus five-dimensional. Target localization parameter identifiability is established with the aid of the Fisher Information Matrix (FIM). The FIM is evaluated for various combinations of the following sequences of measurements: time difference of arrival (TDOA) between the two sensors, depression angles measured at the two sensors, and frequency measurements obtained separately with the two sensors.

The FIM is used to determine bounds on localization performance, and the corresponding uncertainty ellipses associated with the target position are evaluated for various tracking scenarios.

The theoretical results are corroborated by applying a maximum likelihood estimation algorithm to simulated data and observing the results for a series of Monte Carlo simulations.

I. INTRODUCTION

The problem of passively tracking the position of a target in two dimensions has been extensively discussed in the literature [1]-[7]. A performance prediction procedure is developed and applied to the evaluation of a passive *three-dimensional* tracking problem, where the target moves at a constant depth with constant velocity. The position and velocity of the target can be estimated from passive measurements obtained with as few as two sensors which are omnidirectional in the horizontal plane with possible added capability to measure depression angles, in which case they are vertical arrays.

The Fisher Information Matrix (FIM) [10] is evaluated for various combinations of the following sequences of measurements : time difference of arrival (TDOA) between the two sensors, depression angles measured at the two sensors, frequency measurements obtained separately with two sensors. The following issues are addressed:

1) Identifiability - under what conditions (if any) can the target localization parameters be estimated.

2) Assessment of the quality of the parameter estimates via evaluation of the Cramer-Rao Lower Bound (CRLB) of the estimation error covariance [9], [10].

3) Development of a suitable numerical algorithm that yields the

Maximum Likelihood Estimate (MLE) of the parameters by maximizing the likelihood function [10].

4) Comparison of the performance obtained with simulated data to the theoretically predicted CRLB for validation of this approach.

The results demonstrate that reliable estimates of the target position in three dimensions and its velocity can be obtained with measurements such as TDOA between the two sensors and two depression angle measurements. Addition of frequency measurements enhances the accuracy of the estimates. Even with a very limited number of measurements, e.g., six to eight TDOA measurements combined with the depression angle measurements, the target can be localized when in the vicinity of the sensors, i.e, in a region where the observed measurements change noticeably with time. In addition, the results indicate that the near-field estimates obtained from combined TDOA, depression angle and frequency measurements are comparable with bearing measurements, which require additional complexities. The table below summarizes the results for various sensor configurations.

Conf.	TDOA	Freq.	Dep. Ang.	Localization performance
A	X	-	X	Identifiable
B	X	-	-	Practically unidentifiable
C	X	X	X	Identifiable (good performance)
D	-	X	-	Identifiable (marginal performance)
E	X	X	-	Identifiable (better than D)
F	-	X	X	Identifiable
G	-	-	X	Practically unidentifiable

Table 1. Summary of results

Section II discusses the formulation of the target localization problem in three dimensions, and the identifiability condition, stated in terms of the Fisher Information Matrix.

In addition, other measures of performance relating to eigenvalue dispersion and target position uncertainty are also discussed.

Section III deals with the CRLB for target localization which is numerically evaluated for various target trajectories and sequences of measurements.

In Section IV the target localization performance is evaluated experimentally using simulated data in conjunction with a gradient-based Maximum Likelihood algorithm and the errors are compared to the CRLB. The results compare well with the theoretical predictions. Examination of the performance for various test cases provides important insight into the localization accuracy as it depends on the target trajectory relative to the sensor positions and the types of measurements used.

Section V presents a summary and conclusions. The approach is sufficiently general to be applied to air acoustics, passive radar or electromagnetic direction finding.

II. PARAMETER IDENTIFIABILITY AND PERFORMANCE PREDICTIONS.

The target localization information contained in sequences of measurements is examined with the aid of the Fisher Information Matrix. The FIM will be used to determine the CRLB on the error covariance matrix of the target localization parameter vector θ.

The analysis is performed for a three-dimensional case where the target trajectory and the sensors are not in the same plane. In configuration A from Table 1 the passive acoustic sensors (vertical arrays, omnidirectional in the horizontal plane) are placed on the surface of the ocean and the target moves at a constant depth.

The analysis is done for various combinations of the following sequences of measurements :

1) TDOA between the two sensors : $T_d(\theta,t_k)$.

2) Depression angle from sensor i : $A_i(\theta,t_k)$, i=1,2

3) Frequency (Doppler-shifted) at sensor j : $f_j(\theta,t_k)$, j=1,2

II.1 *CRLB for TDOA and Depression Angle Measurements.*

Consider the two sensors represented in Fig.1 with known locations $(x_i, y_i, 0)$, i=1,2. The position of the target at time t_k is given by:

$$x(t_k)=x_0+v_x t_k \qquad \text{(II.1.1)}$$

$$y(t_k)=y_0+v_y t_k \qquad \text{(II.1.2)}$$

$$z(t_k)=z_0 \qquad \text{(II.1.3)}$$

The parameter vector θ, describing the initial position and velocity, is:

$$\theta=(x_o,\ y_o,\ v_x,\ v_y,\ z_o)' \tag{II.1.4}$$

where v_x, v_y, denote the x and y components of the constant velocity vector of the target, and ' denotes vector or matrix transpose. The target moves at a constant depth z_o.

Assuming the TDOA estimates (measurements) $T_d(\theta,t_k)$ are proportional to the corresponding range difference $r_d(\theta,t_k)$ one has

$$T_d=r_d(\theta,t_k)/c \tag{II.1.5}$$

where,

$$r_d(\theta,t_k)=r_1(\theta,t_k)-r_2(\theta,t_k)\triangleq h_1(\theta,t_k)$$

$$=\left\{ \left[x_1-x(t_k) \right]^2+\left[y_1-y(t_k) \right]^2+z_o^2 \right\}^{\frac{1}{2}}$$

$$-\left\{ \left[x_2-x(t_k) \right]^2+\left[y_2-y(t_k) \right]^2+z_o^2 \right\}^{\frac{1}{2}} \tag{II.1.6}$$

and c denotes the speed of sound propagation in the medium. The corresponding range difference measurement $z_1(t_k)$ made with a sensor-pair is given by

$$z_1(t_k)=h_1(\theta,t_k)+w_{z_1}(t_k), \qquad k=1,\ldots,n \tag{II.1.7}$$

where w_{z_1} denotes the measurement noise.

The depression angles are

$$h_2(\theta,t_k)\triangleq A_1(\theta,t_k)$$

$$=\tan^{-1}\left\{ \frac{z_o}{\left[(x_1-x(t_k))^2+(y_1-y(t_k))^2 \right]^{\frac{1}{2}}} \right\} \tag{II.1.8}$$

and,

$$h_3(\theta,t_k)\triangleq A_2(\theta,t_k)$$

$$= \tan^{-1}\left\{ \frac{z_0}{\left[(x_2 - x(t_k))^2 + (y_2 - y(t_k))^2 \right]^{\frac{1}{2}}} \right\} \qquad \text{(II.1.9)}$$

The corresponding measurements made with the sensors are

$$z_2(t_k) = h_2(\theta, t_k) + w_{z_2}(t_k), \qquad k = 1,..,n \qquad \text{(II.1.10)}$$

and,

$$z_3(t_k) = h_3(\theta, t_k) + w_{z_3}(t_k), \qquad k = 1,..,n \qquad \text{(II.1.11)}$$

where w_{z_2}, w_{z_3} denote the angle measurement noises.

Assuming that the measurement noises are independent, identically distributed, normal with zero mean and variances $\sigma_{z_i}^2$, i=1,2,3, the individual likelihood functions of the parameter θ (the joint pdf of the observations $Z_i = [z_i(t_k),\ k = 1,..,n]$, i=1,2,3, conditioned on θ) can be written as:

$$\Lambda_{Z_i}(\theta) = p(Z_i|\theta)$$

$$= \prod_{k=1}^{n} p(Z_i(t_k)|\theta)$$

$$= \alpha_i \exp\left\{ -\frac{1}{2\sigma_{z_i}^2} \sum_{k=1}^{n} \left[z_i(t_k) - h_i(\theta, t_k) \right]^2 \right\} \qquad \text{(II.1.12)}$$

where i=1,2,3 and k=1, . .,n, and α_i denotes the normalization constants.

The covariance of any unbiased estimate $\hat{\theta}(Z)$ of the (non-random) parameter θ cannot be smaller than the CRLB namely

$$P = E\left[(\hat{\theta} - \theta)(\hat{\theta} - \theta)' | \theta \right] \geq \left[J_Z(\theta) \right]^{-1} \qquad \text{(II.1.13)}$$

where

$$J_Z(\theta) = \sum_{i=1}^{3} -E\left[\frac{d^2}{d\theta^2}\ln\Lambda_{Z_i}(\theta)\right] = \sum_{i=1}^{3} J_{Z_i}(\theta) \qquad \text{(II.1.14)}$$

is the FIM corresponding to the combined informational content of the three independent sets of measurements. The Hessian, symbolically written above as the second derivative, is evaluated at the true value of the parameter θ. The additivity follows from the assumption of independence of the measurement noises.

It can be seen that the identifiability condition is equivalent to requiring the FIM to be nonsingular. Otherwise the lower bound is not finite and the parameters are not identifiable.

Using the gradient notation (a column vector) where

$$\nabla_\theta = \left[\frac{d}{dx_o}, \frac{d}{dy_o}, \frac{d}{dv_x}, \frac{d}{dv_y}, \frac{d}{dz_o}\right]' \qquad \text{(II.1.15)}$$

one can evaluate (II.1.14) as follows:

$$\begin{aligned} J_Z(\theta) = & \sum_{i=1}^{3} - E[\nabla_\theta \nabla_\theta' \ln\Lambda_{z_i}(\theta)] \\ & - \sum_{i=1}^{3} \frac{1}{2\sigma_{z_i}^2} E\left\{\sum_{k=1}^{n} \nabla_\theta \nabla_\theta' [z_i(t_k) - h_i(\theta, t_k)]^2\right\} \\ & - \sum_{i=1}^{3} \sigma_{z_i}^{-2} E\left\{\sum_{k=1}^{n} [\nabla_\theta h_i(\theta, t_k)][\nabla_\theta h_i(\theta, t_k)]'\right. \\ & \left. - [\nabla_\theta \nabla_\theta' h_i(\theta, t_k)][z_i(t_K) - h_i(\theta, t_k)]\right\} \end{aligned} \qquad \text{(II.1.16)}$$

Denoting the gradient and Hessian of h as h_θ and $h_{\theta\theta}$, respectively, i.e.,

$$\nabla_\theta h_i(\theta,t_k)\equiv h_{i\theta}(t_k) \tag{II.1.17}$$

$$\nabla_\theta \nabla_\theta' h_i(\theta,t_k)\equiv h_{i\theta\theta}(t_k) \tag{II.1.18}$$

for i=1,2,3 yields

$$J_Z(\theta)=\sum_{i=1}^{3} J_{Z_i}(\theta)$$

$$=\sum_{i=1}^{3}\sigma_{z_i}^{-2}\, E\Big\{\sum_{k=1}^{n} h_{i\theta}(t_k)h_{i\theta}'(t_k)-h_{i\theta\theta}(t_k)[z_i(t_k)-h_i(\theta,t_k)]\Big\} \tag{II.1.19}$$

Since expressions (II.1.17) and (II.1.18) are dterministic, the only stochastic term in (II.1.19) is:

$$z_i(t_k)-h_i(\theta,t_k)= w_{z_i}(t_k) \tag{II.1.20}$$

which was assumed to be zero-mean. Thus (II.1.19) becomes

$$J_Z(\theta)=\sum_{i=1}^{3}\sigma_{z_i}^{-2}\sum_{k=1}^{n} h_{i\theta}(t_k)h_{i\theta}'(t_k) \tag{II.1.21}$$

where it is assumed that the set of TDOA and depression angle measurements are obtained with a single sensor-pair at n discrete instants of time.

A necessary condition for the invertibility of (II.1.21) is that n≥dim(θ)=m, in this case m=5. The analytical expression for (II.1.21) can be obtained from (II.1.6), (II.1.8), and (II.1.9) but at the same time it is too complicated to obtain explicit expression for its invertibility. As discussed in [8] the full rank condition of the set of gradients in (II.1.21) is sufficient for invertibility and thus local identifiability. Since our problem pertains to local identifiability one can work on this condition to obtain the results.

The special structure of (II.1.21) as a sum of dyads implies that it will be invertible iff the set of vectors $h_{i\theta}(t_k)$, k=1,..,n, i=1,2,3,

span the Euclidean space of dimension m=dim(θ).

II.2 *The Identifiability Condition*

To determine target localization parameter identifiability from TDOA and the two depression angle measurements, the gradients $h_{i\theta}(t_k)$, -1,2,3 are evaluated using (II.1.6), (II.1.8) and (II.1.9).

We denote the gradient vectors as follows

$$h_{i\theta}(t_k)=\nabla_\theta h_i(\theta,t_k)=\left[a_{ik},\ b_{ik},\ a_{ik}t_k,\ b_{ik}t_k,\ c_{ik}\right]^{'}, \qquad i=1,2,3 \tag{II.2.1}$$

where the quantities in the last bracket can be obtained explicitly as done in Appendix A. When only TDOA measurements are considered the spanning condition is equivalent to the determinant D_i being non-zero, where

$$|D_i| = \begin{vmatrix} a_{i1} & a_{i2} & a_{i3} & a_{i4} & a_{i5} \\ b_{i1} & b_{i2} & b_{i3} & b_{i4} & b_{i5} \\ a_{i1}t_1 & a_{i2}t_2 & a_{i3}t_3 & a_{i4}t_4 & a_{i5}t_5 \\ b_{i1}t_1 & b_{i2}t_2 & b_{i3}t_3 & b_{i4}t_4 & b_{i5}t_5 \\ c_{i1} & c_{i2} & c_{i3} & c_{i4} & c_{i5} \end{vmatrix} \neq 0, \quad i=1 \tag{II.2.2}$$

Similarly $|D_2|$ and $|D_3|$ can be written corresponding to depression angle measurements by substituting i=2,3 in Eq. (II.2.2), respectively. However, if all the sets of measurements are also considered the determinant of (II.1.21) should be considered. Since the determinant of the sum of matrices is very difficult to evaluate the identifiability will be

discussed in the sequel for one type of measurement at a time. The evaluation of the determinants is relegated to Appendix B.

The conclusions are summarized next. When the target is at endfire, i.e., target bearing angle is zero and target depression angles are also zero, then the gradients are zero, which precludes identifiability. Furthermore in the far-field $B_1(\theta,t_k)\cong B_2(\theta,t_k)$ and $A_1(\theta,t_k)\cong A_2(\theta,t_k)$ which also precludes identifiability. When $B_1(\theta,t_k)+B_2(\theta,t_k)=\pi$, and $A_1(\theta,t_k)=A_2(\theta,t_k)$ i.e., target motion in the perpendicular bisector plane of the segment joining the sensors one has $b_{1k}=0$, $c_{1k}=0$ and the target cannot be practically identified as will be seen later. From the above the near-field condition is necessary for identifiability. The condition for $|D_1|\neq 0$ has been discussed in [7] for a 2-d case. To obtain a similar condition for a 3-d the case is tedious and has been relegated to Appendix B. Thus, with the 5-dimensional parameter vector for a target moving in a 3-dimensional space one has practical identifiability from TDOA and depression angle measurements unless:

1) Target at endfire or far-field.

2) Target motion in the perpendicular bisector plane of the segment joining the two sensors.

II.3 *CRLB for the Combination of Complementary Measurements.*

The contribution of additional measurements made with a pair of sensors, such as single-sensor target frequency estimates (measurements), which are

denoted with i=4,5 as

$$f_j(\theta,t_k) \triangleq h_i(\theta,t_k) = [1+\dot{r}_{i-3}(\theta,t_k)/c]f_0 \qquad i=4,5 \qquad j=1,2 \tag{II.3.1}$$

where $\dot{r}_{i-3}(\theta,t_k)$ denotes the time derivative of the range measured by the respective sensor, c denotes the speed of sound propagation in the medium and f_0 denotes the Doppler-free target frequency. The corresponding measurements are

$$z_i(t_k) = h_i(\theta,t_k) + w_{z_i}(t_k) \qquad i=1,2 \tag{II.3.2}$$

where w_{z_i} is the measurement noise, which is white, with zero mean and a variance $\sigma_{z_i}^2$.

The total FIM $J_2(\theta)$, corresponding to all the sets of measurements obtained with a pair of sensors, is given by

$$J_2(\theta) = \sum_{i=1}^{5} \sigma_{z_i}^{-2} \sum_{k=1}^{n} h_{i\theta}(t_k) h_{i\theta}'(t_k) \tag{II.3.3}$$

where $h_{i\theta}(t_k)$ denotes the gradient of $h_i(\theta,t_k)$ as defined earlier in Eq. (II.1.17).

II.4 Additional Performance Measures.

The inverse of FIM is the CRLB for the error coavriance matrix P associated with the target localization parameter estimates i.e.,

$$P \geq J^{-1}(\theta) \tag{II.4.1}$$

where $J^{-1}(\theta)$ denotes the FIM for the combination of multiple measurement sets. The determinant of $J^{-1}(\theta)$ provides a measure of the lower bound of the hypervolume of the multiple dimensional uncertainty ellipsoid [10], associated with target localization parameter estimate. The shape of the

uncertainty ellipsoid can be obtained from the solution of the eigensystem involving $J^{-1}(\theta)$. The eigensystem provides the following interpretations: i) The lengths of the axes and their orientation in the reference coordinate system are given by the corresponding eigenvalues and eigenvectors, i.e.,

$$J^{-1}(\theta)E_i = \lambda_i E_i \tag{II.4.2}$$

where E_i and λ_i are the eigenvectors and the corresponding eigenvalues, respectively. ii) The dispersion of the eigenvalues, $\lambda_{max} / \lambda_{min}$, also provides a measure of parameter identifiability [7].

The uncertainty ellipse for the target's horizontal position at time t can be easily derived from $J^{-1}(\theta)$ as follows. The predicted position for time t is

$$\begin{bmatrix} x(t) \\ y(t) \end{bmatrix} = \begin{bmatrix} 1 & 0 & t & 0 & 0 \\ 0 & 1 & 0 & t & 0 \end{bmatrix} \theta \tag{II.4.3}$$

One can obtain the corresponding position error covariance matrix corresponding to time t, $C_p(\theta,t)$ as:

$$C_p(\theta,t) = \begin{bmatrix} 1 & 0 & t & 0 & 0 \\ 0 & 1 & 0 & t & 0 \end{bmatrix} J^{-1}(\theta) \begin{bmatrix} 1 & 0 \\ 0 & 1 \\ t & 0 \\ 0 & t \\ 0 & 0 \end{bmatrix} \tag{II.4.4}$$

The shape and area of this position uncertainy ellipse can be obtained from the appropriate eigensystem solution.

III. PERFORMANCE PREDICTIONS

The performance measures discussed in Section II, i.e., identifiability, matrix or data ill-conditioning, the area and elongation of the ellipse, are determined for various situations in this section. Five scenarios of target trajectory and sensor configurations were chosen to determine the feasibility of target localization using measurements from a pair of sensors. Using sequences of TDOA, depression angles and/or frequency measurements, questions of identifiability, matrix ill-conditioning, and target parameter uncertainty will be addressed with the aid of *FIM*.

Case I

The first case consists of a target trajectory making an angle of 45^0 with the array axis as shown in Fig.2a. The target passes between the sensors spaced 2 km. The target location in this case is generally identifiable, from TDOA and depression angle measurements (sensor configuration A from Table 1). The FIM was determined for a constant speed of 10 kn using a sequence of eight TDOA and depression angle measurements corresponding to the eight equispaced target positions indicated in Fig.2a. The target is assumed to be moving at a depth of 0.2 km. The FIM was evaluated and found to be non-singular with a conditioning measure, $\log_{10}(\lambda_{max}/\lambda_{min})=7.78$. The standard deviations of TDOA and depression angles are 0.1s and 6^0 respectively. The area of the corresponding two-sigma horizontal position uncertainty ellipse, shown in Fig.2a corresponding to the largest ellipse is 0.9 km^2. Under the Gaussian assumption, the positional estimate will fall within this ellipse

with 86.5 % probability. The depth standard deviation was 0.04 km. The addition of frequency measurements to the above measurements (configuration C) further improves the performance. The zero-Doppler frequency is 100 Hz. The standard deviation of frequency measurements was 0.1Hz. The corresponding conditioning measure was 7.55 and the largest area of the corresponding two-sigma position uncertainty ellipse was 0.615 km^2 as shown in Fig. 2b and the depth standard deviation was 0.0358 km. Using only TDOA and depression angle measurements with the latter more accurate to $\sigma=3^0$ resulted in a considerable improvement in the performance measure. The corresponding values for the conditioning measure and for the area of the largest two-sigma uncertainty ellipse are 6.96 and 0.319 km^2 respectively. The results are shown in Fig.2c and the depth standard deviation was 0.0348 km.

It is interesting to note that results from Fig.2a when compared to those from [7] show that for these numbers the 3-d problem with TDOA and depression angles yields better accuracy than the 2-d problem with TDOA measurements only.

Case II

The second case examined consists of a target trajectory that is perpendicular to the array axis and intersecting the axis at a point outside the sensors as shown in Fig.3a. Configuration A namely, TDOA and the two depression angle measurements was considered. The FIM was very ill-conditioned and the uncertainty areas are too large. The addition of frequency measurements (configuration C) significantly improves target localization. The FIM was first obtained for the TDOA and the two depression angle measurements (configuration A), each set

consisting of eight samples. For a target speed of 10 kn and the sensors spaced 2 km apart, the matrix conditioning measure is 7.18 and the area of the two-sigma position uncertainty ellipse shown in Fig.3a is 1.6 km^2 and the depth standard deviation was 0.0634 km. The addition of two sets of frequency measurements and all the other quantities remaining the same (configuration C), gave a matrix conditioning measure of 6.48, and the area of the two-sigma position uncertainty ellipse as 0.496km^2 respectively, as shown in Fig.3b and the depth standard deviation was 0.05698 km.

Case III

The third case examined consists of a target trajectory that is parallel to the array axis. Evaluation of the FIM based on the TDOA and the depression angle measurements (configuration A) indicated still poor localization as in Case II. This is illustrated in Fig.4a. Localizability can be improved by the addition of the frequency measurements (configuration C). The FIM was obtained for combined sets of TDOA and depression angle measurements consisting of eight samples each and sets of TDOA, depression angles and frequency measurements, consisting of eight samples each. The matrix conditioning measure and area of the two-sigma position uncertainty ellipse as shown in Fig.4a. and Fig.4b are 7.43, and 1.357 km^2 (configuration A) respectively, and 5.98 and 0.438 km^2 (configuration C) respectively, and the depth standard deviations were 0.099 km and 0.089 km, respectively.

Case IV

The fourth case consists of a target trajectory perpendicular to the array axis passing through the individual sensors and equidistant to the two sensors spaced at 2 km i.e., in the perpendicular bisector plane. The FIM was evaluated on the basis of TDOA and depression angle estimates (configuration A). Regardless of target initial position along this trajectory or target speed, a constant TDOA sequence of zero results. The target localization parameters are practically unidentifiable if based on TDOA and depression angle measurements alone, as shown in Fig.5a. To localize a target with this trajectory, it is necessary to obtain additional measurements. Frequency measurements obtained with each of the sensors were used in conjunction with the TDOA and depression angle measurements (configuration C). The FIM was evaluated for the combined five sets of measurements. The matrix conditioning measure is 6.73, which although relatively large, produces resonable results. The corresponding two-sigma position uncertainty ellipse illustrated in Fig.5b has an area of 0.205km^2 and the depth standard deviation was 0.0367 km. The FIM was also evaluated for depression angle measurements only (configuration G) and the target was found to be practically unidentifiable. The standard deviation of the depression angle measurements was 6^0. The conditioning measure was 6.73 and the area of the two-sigma uncertainty ellipse was 17.41 km^2 as shown in Fig.5c with the depth standard deviation of 0.0583 km. Finally the FIM was evaluated for frequency measurements only obtained separately with the two sensors (configuration D). The standard deviation of the frequency measurements was 0.1Hz. The resulting conditioning measure was 7.45 and the area of the two-sigma uncertainty ellipse was 2.59 km^2 as shown in Fig.5d, while the

depth standard deviation was 4.46 km. The horizontal localization uncertainty is not too large but this measurement carries practically no information about depth.

Case V

In this case the target trajectory was as in Case I but the types of measurements are different. The FIM was evaluated using only the target frequency measurements obtained separately with two sensors (configuration D). The results revealed that the target is generally identifiable as shown in Fig.6a. Addition of depression angle measurements (configuration F) improved performance as shown in Fig.6b. The conditioning measure and the area of the largest two-sigma uncertainty ellipse are 7.097, and 0.805 km^2, respectively, for (configuration D) and the depth standard deviation was 2.16 km; and 6.74 and 0.325 km^2, respectively, (configuration F) as in Fig.6b. and the depth standard deviation was 0.0384 km respectively. Finally the FIM was evaluated by assuming only TDOA and frequency measurements (configuration E). The target is identifiable and the corresponding matrix conditioning measure is 7.467 and the area of the two-sigma position uncertainty ellipse as in Fig.6c. is 0.203 km^2 and the depth standard deviation was 1.211 km.

Note that in all the above cases that have been evaluated the target's direction of travel along the constant velocity trajectory does not affect the results of the analysis.

IV. VALIDATION OF THE PERFORMANCE PREDICTION TECHNIQUE.

Experimental performance evaluation was done with the implementation of a maximum likelihood parameter estimation algorithm by using simulated measurement data. The algorithm uses the Conjugate Gradient Search method to minimize the least squares criterion equivalent to the maximum likelihood. In this algorithm the error measure is the difference between the noisy measurement data and measurement predictions based on the estimated localization parameter values. Simulated data consisting of TDOA, depression angle and frequency measurements were formed for one selected scenario. The measurement data were corrupted by additive white Gaussian noise of a known variance. For one scenario as in Case I, 50 Monte Carlo tracking simulations were made to form a statistical base for examination of the localization error. The resulting localization estimates were then plotted, forming scatter diagrams indicative of the algorithm's performance. The corresponding two-sigma error ellipse as predicted by the FIM's were superimposed over the scatter plots, allowing for a direct comparison between the experimental and the theoretically predicted performance. The results are shown in Fig.8. For the 50 tests performed, good agreement exists between the experimental results and the theoretical uncertainty ellipses shown. A sequence of uncertainty ellipses and the corresponding scatter diagrams are shown in the figure for the duration of the target path from which measurements were obtained.

V. SUMMARY AND CONCLUSIONS

Following the earlier work [7], where the analysis was done for a two-dimensional tracking problem with two omnidirectional sensors, in this work the analysis has been extended to a three-dimensional tracking problem with two sensors. An analysis procedure based on the information contained in various sets of measurements, viz. the TDOA, the two depression angles, and the target frequencies measured separately with the two sensors has been developed and tested for evaluation of target localization with a pair of sensors, when the target moves in the vicinity of the sensors. This tool was initially used to determine if the informational content of a set of measurements is sufficient to identify the localization parameters. The analysis also yields important performance measures such as algorithm convergence indicators, position and velocity parameter uncertainty ellipses for a three-dimensional passive tracking problem. Examination of the performance for various test cases provided insight relating localization accuracy to target trajectory relative to sensor positions, measurement types and measurement quality. The results demonstrate that reliable localization based on TDOA and depression angle measurements occurs primarily for targets passing between the sensors. The TDOA measurements in conjunction with the depression angle measurements were observed to yield a somewhat elongated position uncertainty ellipse. The simultaneous use of all types of measurements, i.e., frequency, TDOA, and depression angle produced an improved uncertainty ellipse in terms of eigenvalue dispersion.

A more interesting finding is that a target in motion in 3-dimensions can be localized by using only the target frequency measurements obtained separately with two sensors.

The results of the computer simulations are in good agreement with the theoretical performance predictions obtained with the CRLB. The following important results can be stated :

1) A target in motion in three dimensions can be localized by evaluating the TDOA and depression angle measurements (configuration A) obtained with two sensors, unless the target is at endfire or far-field. Motion in the perpendicular bisector plane is practically not identifiable.

2) A target in motion in 3-dimensions cannot be practically localized by evaluating only the TDOA measurements (configuration B) obtained with two sensors. However, it can be localized by evaluating only the target frequency measurements obtained separately with two sensors (configuration D). Any additional measurements like the TDOA or the depression angle measurements improve performance.

The analysis is general and can be applied to air acoustics, passive radar, and electromagnetic direction finding. With such an analysis tool one can predict performance, i.e., the ability to track, and separate targets, for various types and qualities of measurements. This analysis indicates the potential of a field of sensors in tracking targets.

Acknowledgement

Stimulating discussions with Dr. D Gingras of NOSC (ONR) are gratefully acknowledged.

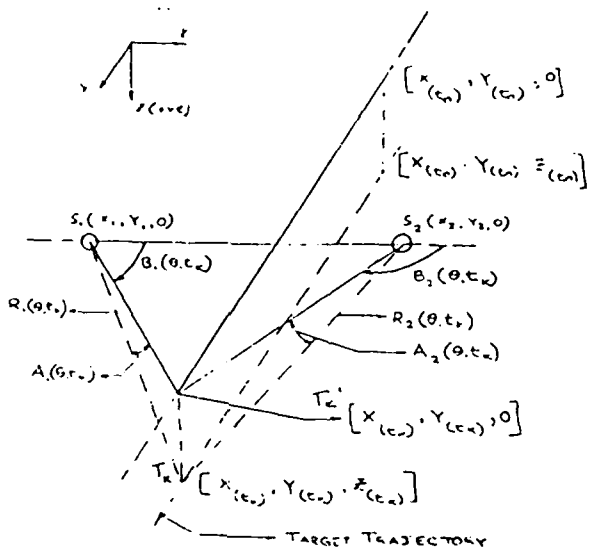

Fig. 1. Notation for target trajectory, sensor positions, corresponding localization parameters, and depression angles and range measurements.

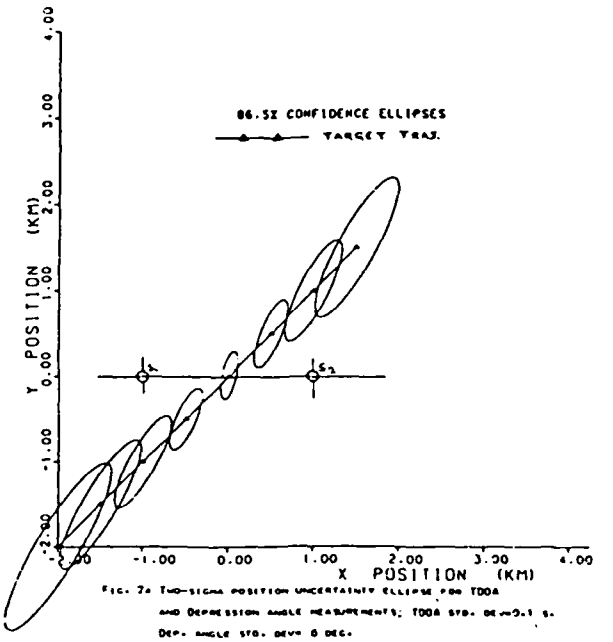

FIG. 2a TWO-SIGMA POSITION UNCERTAINTY ELLIPSE FOR TDOA AND DEPRESSION ANGLE MEASUREMENTS; TDOA STD. DEV=0.1 μs, DEP. ANGLE STD. DEV= 0 DEG.

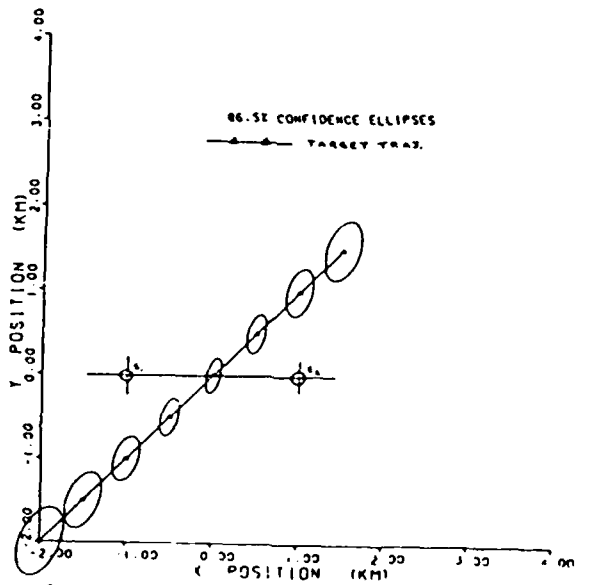

FIG. 2b UNCERTAINTY ELLIPSE FOR CASE I TRAJECTORY WITH TDOA, DEPRESSION ANGLE AND FREQUENCY MEASUREMENTS; $\sigma_{\tau_{21}}$=0.1 μs, $\sigma_{\theta_{21}}$=0 DEG., σ_f =0.1 Hz, ZERO-DOPPLER SHIFT FREQUENCY = 100 Hz.

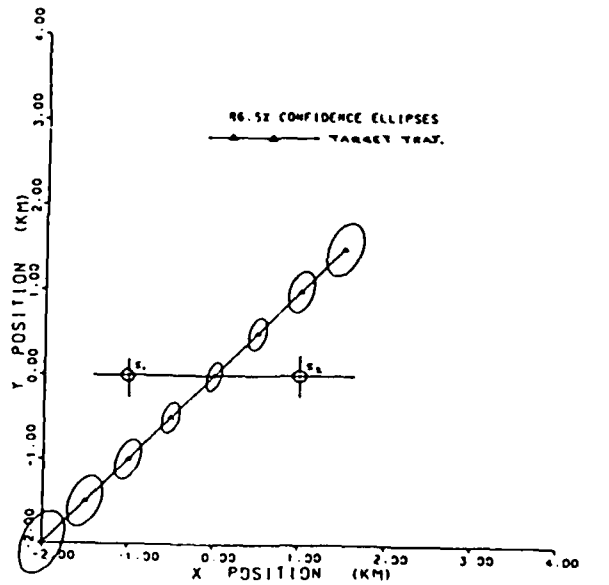

FIG. 2c UNCERTAINTY ELLIPSE FOR CASE I TRAJECTORY WITH TDOA, DEPRESSION ANGLE AND FREQUENCY MEASUREMENTS; $\sigma_{\tau_{21}}$=0.1 μs, $\sigma_{\theta_{21}}$ = 1 DEG, σ_f =0.1 Hz, ZERO-DOPPLER SHIFT FREQUENCY = 100 Hz.

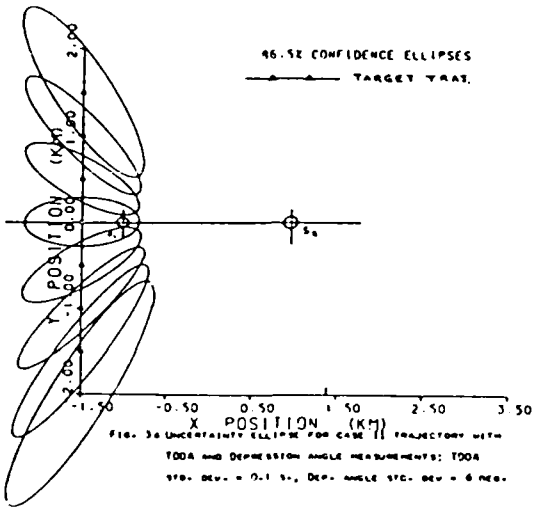

Fig. 3a Uncertainty ellipse for case II trajectory with TDOA and depression angle measurements; TDOA std. dev. = 0.1 s., Dep. angle std. dev = 6 deg.

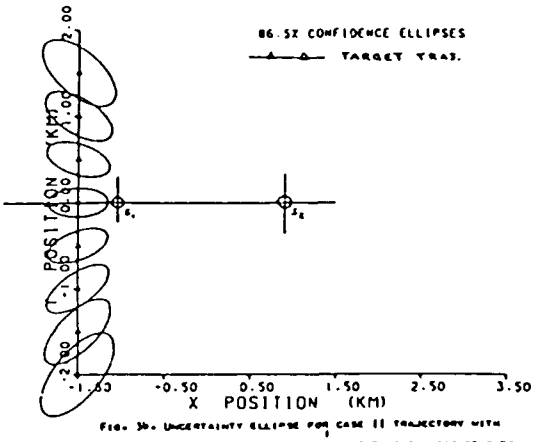

Fig. 3b. Uncertainty ellipse for case II trajectory with TDOA, Depression angle and frequency measurements; $\sigma_{t_{21}}$=0.1s., $\sigma_{\theta_{dep}}$=6 deg., σ_f =0.1 Hz. Zero-doppler shift frequency=100Hz.

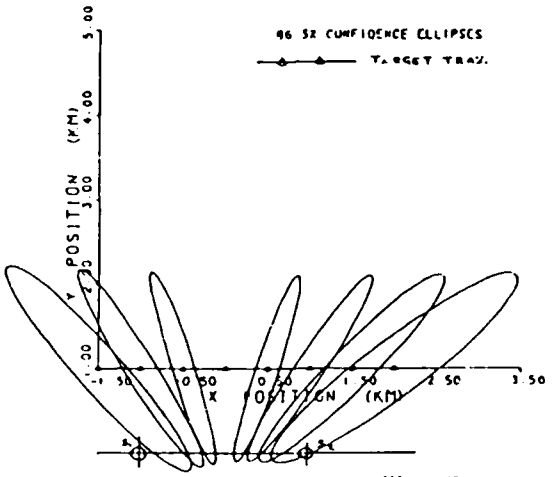

Fig. 4a Uncertainty ellipse for case III trajectory with TDOA and Depression angle measurements; TDOA std. dev. = 0.1 s., Dep. angle std. dev.=6 deg.

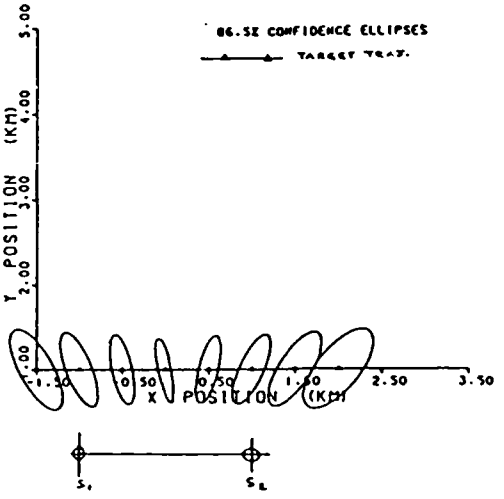

Fig. 4b. Uncertainty ellipse for case III trajectory with TDOA, Depression angle and frequency measurements; $\sigma_{t_{21}}$=0.1s., $\sigma_{\theta_{dep}}$=6 deg., σ_f =0.1Hz. Zero-doppler frequency=100Hz.

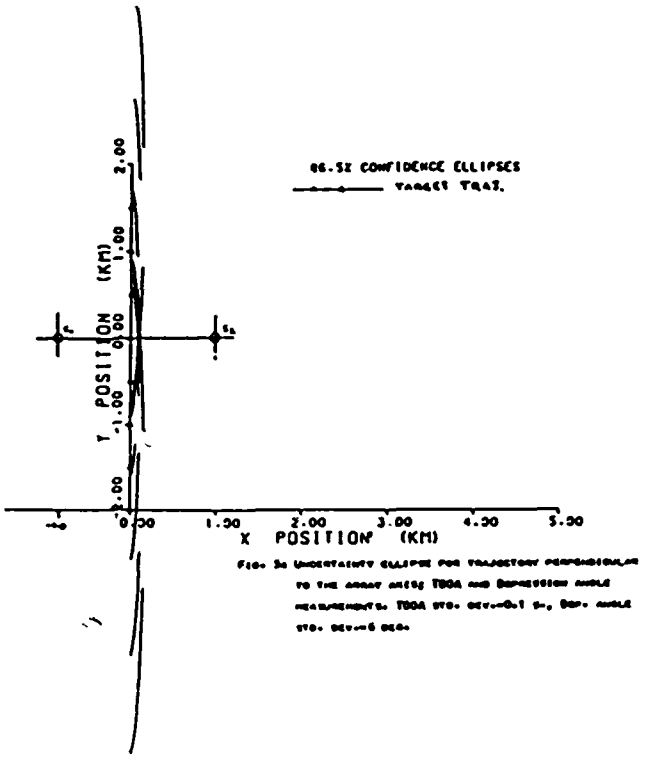

FIG. 5a UNCERTAINTY ELLIPSE FOR TRAJECTORY PERPENDICULAR TO THE ARRAY AXES TDOA AND DEPRESSION ANGLE MEASUREMENTS. TDOA STD. DEV.=0.1 μs, DEP. ANGLE STD. DEV.=6 DEG.

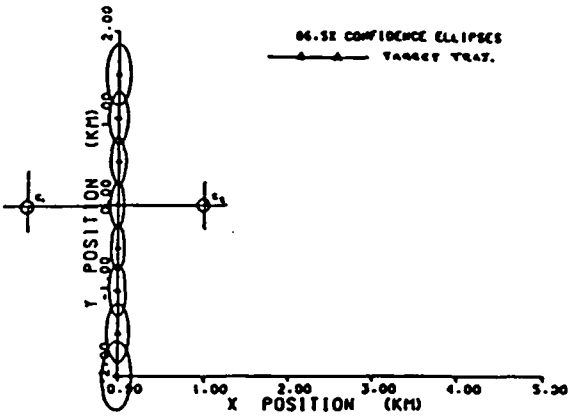

FIG. 5b. UNCERTAINTY ELLIPSE FOR TRAJECTORY PERPENDICULAR TO ARRAY AXES WITH TDOA, DEPRESSION ANGLE AND FREQUENCY MEASUREMENTS, σ_{t_d} =0.1μs, σ_{θ_d} =6 DEG. σ_f =0.1HZ., ZERO-DOPPLER FREQUENCY=100HZ.

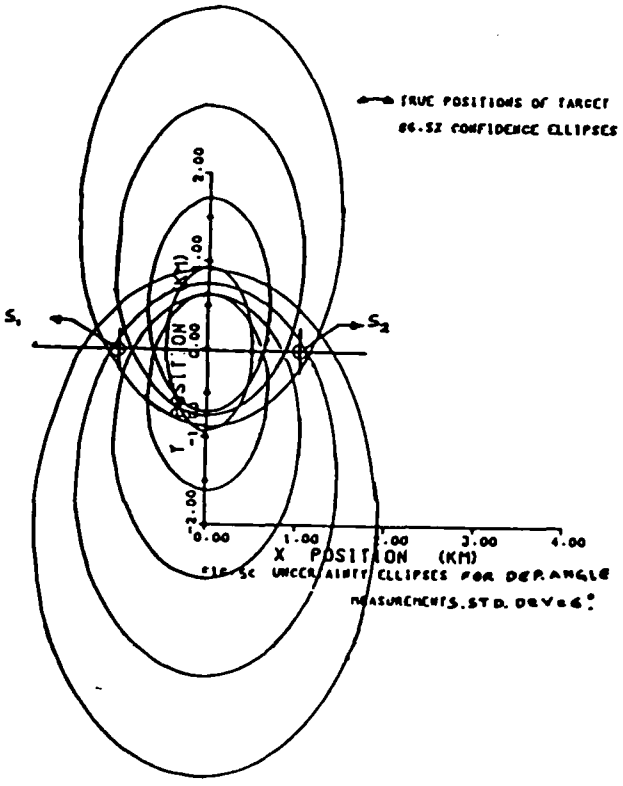

FIG. 5c UNCERTAINTY ELLIPSES FOR DEPANGLE MEASUREMENTS, STD. DEV=6°

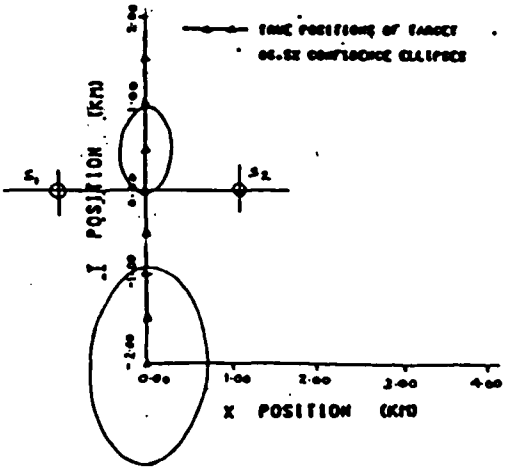

FIG. 5d UNCERTAINTY ELLIPSES FOR FREQUENCY MEASUREMENTS ONLY, STD. DEV. OF FREQUENCY MEASUREMENTS 0.1 HZ. DOPPLER SHIFT FREQUENCY=100 HZ

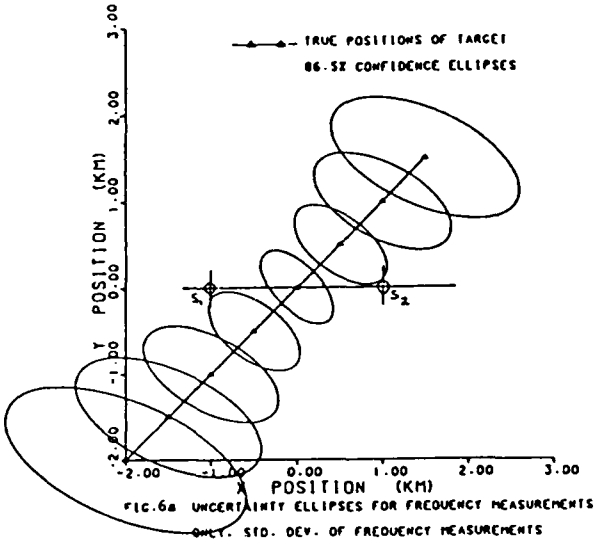

FIG.6a UNCERTAINTY ELLIPSES FOR FREQUENCY MEASUREMENTS ONLY. STD. DEV. OF FREQUENCY MEASUREMENTS =0.1 HZ. DOPPLER SHIFT FREQUENCY=100 HZ

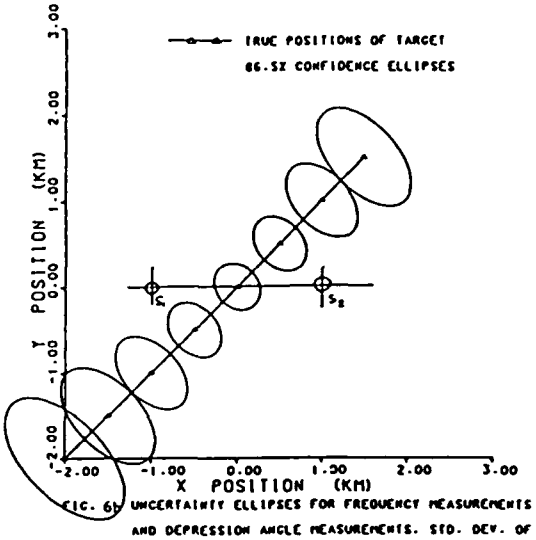

FIG. 6b UNCERTAINTY ELLIPSES FOR FREQUENCY MEASUREMENTS AND DEPRESSION ANGLE MEASUREMENTS. STD. DEV. OF FREQUENCY=0.1 HZ. STD. DEV. OF DEP. ANG.=6 DEG. ZERO-DOPPLER SHIFT FREQUENCY=100 HZ

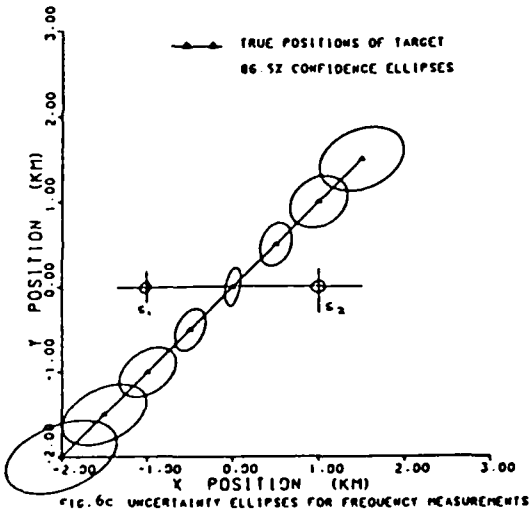

FIG.6c UNCERTAINTY ELLIPSES FOR FREQUENCY MEASUREMENTS AND TDOA MEASUREMENTS. STD. DEV. OF FREQ.=0.1HZ STD. DEV. OF TDOA=0.1 SEC. ZERO-DOPPLER SHIFT FREQUENCY=100 HZ

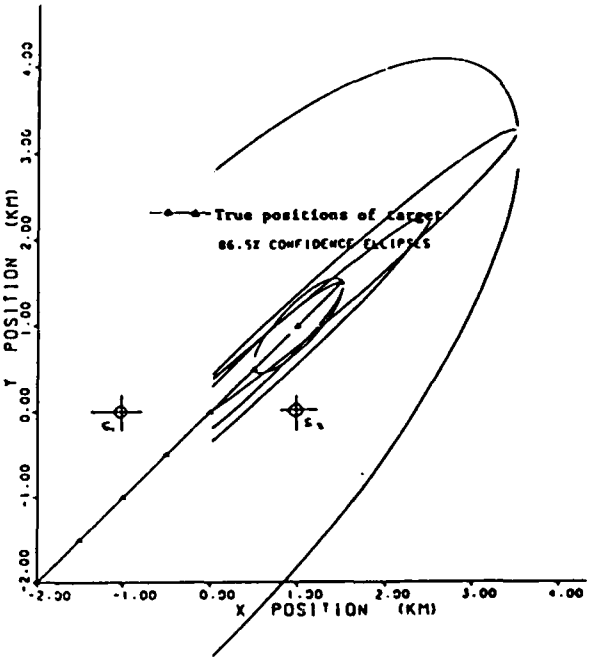

Fig. 7 Uncertainty ellipses for only TDOA measurements, Std. Dev. of TDOA=0.1 sec.

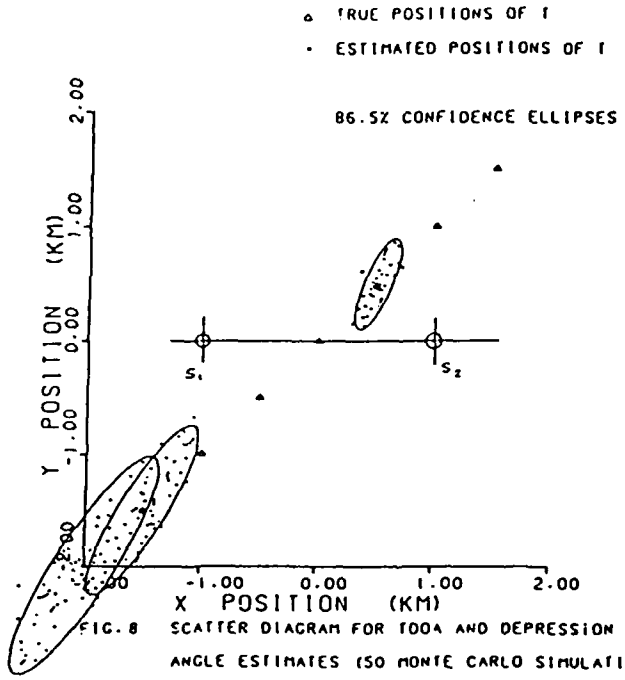

FIG. 8 SCATTER DIAGRAM FOR TDOA AND DEPRESSION ANGLE ESTIMATES (50 MONTE CARLO SIMULATIONS)

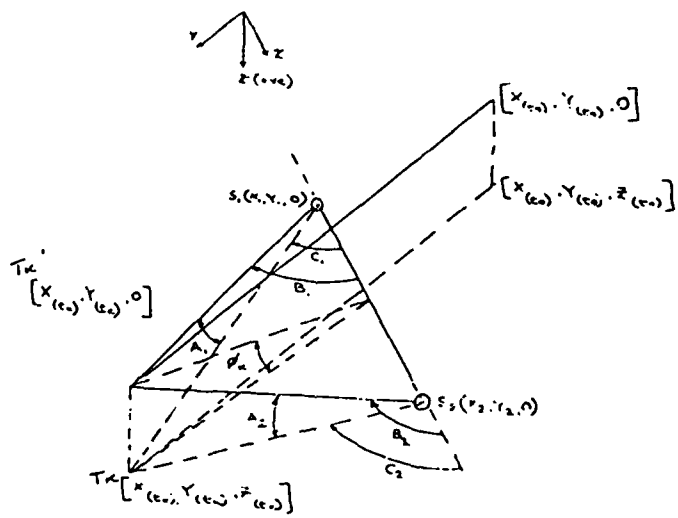

C_1, C_2 = Conical bearing angle of the target w.r. to the two sensors.

ϕ_k = Angle between $T_k'N$ and T_kN;

$\cos C_1 = \cos B_1 \cos A_1$; $\cos \phi_k \sin C_1 = \sin B_1 \cos A_1$

Fig. B4. Notation for target trajectory, and additional angles. ϕ_k & $C_i(\theta, t_k)$, $i = 1,2$

APPENDIX A

Evaluation of Gradients - $h_{i\theta}(t_k)$

To determine target localization identifiability from TDOA and the two depression angle estimates, the gradients of $h_i(\theta,t_k)$, i=1,2,3 are evaluated using equations (II.1.6), (II.1.8) and (II.1.9) in Section II, as follows:

$$\frac{d}{dx_0}h_i(\theta,t_k) = -\frac{x_1-x(t_k)}{r_1(\theta,t_k)} + \frac{x_2-x(t_k)}{r_2(\theta,t_k)}$$

$$= \left\{\frac{x(t_k)-x_1}{\rho_1(\theta,t_k)}\right\}\left\{\frac{\rho_1(\theta,t_k)}{r_1(\theta,t_k)}\right\} - \left\{\frac{x(t_k)-x_2}{\rho_2(\theta,t_k)}\right\}\left\{\frac{\rho_2(\theta,t_k)}{r_2(\theta,t_k)}\right\}$$

$$= \cos B_{1k}\cos A_{1k} - \cos B_{2k}\cos A_{2k}$$

$$= a_{1k} \qquad \text{(A.1)}$$

where

$$\rho_1(\theta,t_k) = \left[(x_1-x(t_k))^2+(y_1-y(t_k))^2\right]^{\frac{1}{2}} \qquad \text{(A.2)}$$

and,

$$\rho_2(\theta,t_k) = \left[(x_2-x(t_k))^2+(y_2-y(t_k))^2\right]^{\frac{1}{2}} \qquad \text{(A.3)}$$

and B_{1k} and B_{2k} denote the bearing angles at time

t_k measured with respect to a plane passing through the two sensors and the target. Similarly

$$\frac{d}{dy_0}h_1(\theta,t_k) = \sin B_{1k}\cos A_{1k} - \sin B_{2k}\cos A_{2k}$$

$$= -b_{1k} \tag{A.4}$$

$$\frac{d}{dz_0}h_1(\theta,t_k) = \frac{z_0}{r_1(\theta,t_k)} - \frac{z_0}{r_2(\theta,t_k)}$$

$$= \sin A_{1k} - \sin A_{2k}$$

$$= c_{1k} \tag{A.5}$$

$$\frac{d}{dv_x}h_1(\theta,t_k) = a_{1k}t_k \tag{A.6}$$

$$\frac{d}{dv_y}h_1(\theta,t_k) = b_{1k}t_k \tag{A.7}$$

Similarly gradients of $h_2(\theta,t_k)$ and $h_3(\theta,t_k)$ are

$$\frac{d}{dx_0}h_2(\theta,t_K) = \frac{d}{dx_0}\tan^{-1}\left\{\frac{z_0}{\left[(x_1-x(t_k))^2+(y_1-y(t_k))^2\right]^{\frac{1}{2}}}\right\}$$

$$= \left\{\frac{z_0}{r_1(\theta,t_k)^2}\right\}\left\{\frac{(x_1-x(t_k))}{\rho_1(\theta,t_k)}\right\}$$

$$= \frac{\sin A_{1k}}{r_1}(-\cos B_{1k})$$

$$= a_{2k} \tag{A.8}$$

$$\frac{d}{dy_0}h_2(\theta,t_k) = \frac{d}{dy_0}\tan^{-1}\left\{\frac{z_0}{\left[(x_1-x(t_k))^2+(y_1-y(t_k))^2\right]^{\frac{1}{2}}}\right\}$$

$$= \frac{\sin A_{1k}}{r_1}(-\sin B_{1k})$$

$$= -b_{2k} \tag{A.9}$$

$$\frac{d}{dz_0}h_2(\theta,t_k) = \frac{d}{dz_0}\tan^{-1}\left\{\frac{z_0}{\left[(x_1-x(t_k))^2+(y_1-y(t_k))^2\right]^{\frac{1}{2}}}\right\}$$

$$= \frac{\rho_1}{r_1^2}$$

$$= \frac{\cos A_{1k}}{r_1}$$

$$= c_{2k} \tag{A.10}$$

$$\frac{d}{dv_x}h_2(\theta,t_k) = a_{2k}t_k \tag{A.11}$$

$$\frac{d}{dv_y}h_2(\theta,t_k) = b_{2k}t_k \tag{A.12}$$

$$\frac{d}{dx_0}h_3(\theta,t_k) = \left\{\frac{z_0}{r_2(\theta,t_k)^2}\right\}\left\{\frac{x_2-x(t_k)}{\rho_2(\theta,t_k)}\right\}$$

$$= \frac{\sin A_{2k}}{r_2}(-\cos B_{2k})$$

$$= -a_{3k} \tag{A.13}$$

$$\frac{d}{dy_0}h_3(\theta,t_k) = \left\{\frac{z_0}{r_2(\theta,t_k)^2}\right\}\left\{\frac{y_2-y(t_k)}{\rho_2(\theta,t_k)}\right\}$$

$$= \frac{\sin A_{2k}}{r_2}(-\sin B_{2k})$$

$$= -b_{3k} \tag{A.14}$$

$$\frac{d}{dz_0}h_3(\theta,t_k) = \frac{\rho_2}{r_2^2}$$

$$= -\frac{\cos A_{2k}}{r_2}$$

$$= -c_{3k} \tag{A.15}$$

$$\frac{d}{dv_x}h_3(\theta,t_k) = -a_{3k}t_k \tag{A.16}$$

$$\frac{d}{dv_y}h_3(\theta,t_k) = -b_{3k}t_k \tag{A.17}$$

If the frequency measurements are also considered the gradients of h_i, i=4,5 are evaluated using the Eq. (II.3.1), i.e.

$$\frac{d}{dx_0}h_i(\theta,t_k) = \frac{f_0}{c}\left\{\frac{v_x}{r_j} - \frac{1}{r_j^3}\left[v_x(x_j-x(t_k))^2+v_y(y_j-y(t_k)(x_j-x(t_k))\right]\right\}$$

$$= a_{ik}, \qquad i=4,5; \qquad j=1,2 \tag{A.18}$$

$$\frac{d}{dy_0} h_i(\theta,t_k) = \frac{f_0}{c}\left\{\frac{v_y}{r_j} - \frac{1}{r_j^3}\left[v_x(x_j-x(t_k))(y_j-y(t_k))+v_y(y_j-y(t_k))^2\right]\right\}$$

$$= b_{ik}, \qquad i=4,5; \qquad j=1,2 \tag{A.19}$$

$$\frac{d}{dz_0} h_i(\theta,t_k) = \frac{f_0 z_0}{c}\left[\frac{v_x(x_j-x(t_k))+v_y(y_j-y(t_k))}{r_j^3}\right]$$

$$= c_{ik}, \qquad i=4,5 \qquad j=1,2 \tag{A.20}$$

$$\frac{d}{dv_x} h_i(\theta,t_k) = -\frac{f_0}{c}\left\{\frac{(x_j-x_0-2v_x t_k)}{r_j} + \frac{\left[v_x(x_j-x(t_k))+v_y(y_j-y(t_k))\right](x_j-x(t_k))t_k}{r_j^3}\right\},$$

$$= d_{ik}, \qquad i=4,5; \qquad j=1,2 \tag{A.21}$$

$$\frac{d}{dv_y} h_i(\theta,t_k) = -\frac{f_0}{c}\left\{\frac{(y_j-y_0-2v_y t_k)}{r_j} + \frac{\left[v_x(x_j-x(t_k))+v_y(y_j-y(t_k))\right](y_j-y(t_k))t_k}{r_j^3}\right\},$$

$$= e_{ik}, \qquad i=4,5; \qquad j=1,2 \tag{A.22}$$

Thus the gradient vectors $h_{i\theta}(\theta,t_k)$, $i=1,2,3,4,5$ are given by:

$$h_i(\theta,t_k) = \nabla_\theta h_i(\theta,t_k)$$

$$= [\,a_{ik},\ b_{ik},\ a_{ik}t_k,\ b_{ik}t_k,\ c_{ik}\,]' \tag{A.23}$$

APPENDIX B

Identifiability Conditions for the 3-d case

The identifiability condition is evaluated in two steps:

1) To prove the identifiability of the corresponding system only for TDOA estimates.

2) Apply the approach in step (1) to the general problem where the TDOA and depresssion angle estimates are considered. [In addition the complementary measurement sets may also be considered.]

B.1 Step 1- only TDOA measurements considered.

In this case one has now to show that the determinant of the matrix D_1 is non-zero. Using the relation $t_k = (k-1)\Delta$, $|D_1|$ reduces as follows:

$$|D_1| = \begin{vmatrix} a_{11} & a_{12} & a_{13} & a_{14} & a_{15} \\ b_{11} & b_{12} & b_{13} & b_{14} & b_{15} \\ c_{11} & c_{12} & c_{13} & c_{14} & c_{15} \\ 0 & a_{12}\Delta & a_{13}2\Delta & a_{14}3\Delta & a_{15}4\Delta \\ 0 & b_{12}\Delta & b_{13}2\Delta & b_{14}3\Delta & b_{15}4\Delta \end{vmatrix} \qquad \text{(B.1.1)}$$

This determinant can be developed along the first column from which one can deduce that $|D_1|$ can be zero if

1) $a_{11} = 0$ and, (B.1.2)

2) $b_{11} = 0$ and, (B.1.3)

3) $c_{11} = 0$ (B.1.4)

which further implies that

1) $a_{1k} = 0$ and, (B.1.5)

2) $b_{1k} = 0$ and, (B.1.6)

3) $c_{1k} = 0$ (B.1.7)

{This follows from the fact that $|D_1|$ can be developed along any column. Also, k=1,..,5, since the minimum number of measurements are considered.}

$$a_{1k} = 0 \Rightarrow \cos B_{1k}\cos A_{1k} - \cos B_{2k}\cos A_{2k} = 0 \quad \text{(B.1.8)}$$

$$b_{1k} = 0 \Rightarrow \sin B_{1k}\cos A_{1k} - \sin B_{2k}\cos A_{2k} = 0 \quad \text{(B.1.9)}$$

$$c_{1k} = 0 \Rightarrow \sin A_{1k} - \sin A_{2k} = 0 \quad \text{(B.1.10)}$$

The above three conditions imply the following: When $B_1(\theta, t_k) = B_2(\theta, t_k)$ and $A_1(\theta, t_k) \cong A_2(\theta, t_k)$ one has $h_1(\theta, t_k) = 0$. Thus a measurement does not provide any information, when the target is at endfire. Furthermore, in the far-field $B_1(\theta, t_k) \cong B_2(\theta, t_k)$ and $A_1(\theta, t_k) \cong A_2(\theta, t_k)$ and all the gradients are practically zero, which, as intuitively expected, precludes identifiability. In other words *the near-field condition is necessary for identifiability.* When $B_1(\theta, t_k) + B_2(\theta, t_k) = \pi$, and $A_1(\theta, t_k) = A_2(\theta, t_k)$ i.e., along the perpendicular bisector plane of the line joining the two sensors, one has $b_{1k} = 0$ and $c_{1k} = 0$ and motion along this perpendicular bisector plane also precludes identifiability.

In addition for determinant of D_1 to be zero the following have to be simultaneously zero i.e.,

4) $|D_{bc}| = 0$, and (B.1.11)

5) $|D_{ac}| = 0$, and (B.1.12)

6) $|D_{ab}| = 0$ (B.1.13)

where

$$D_{bc} = \begin{bmatrix} b_{12} & b_{13} & b_{14} & b_{15} \\ c_{12} & c_{13} & c_{14} & c_{15} \\ a_{12}\Delta & a_{13}2\Delta & a_{14}3\Delta & a_{15}4\Delta \\ b_{12}\Delta & b_{13}2\Delta & b_{14}3\Delta & b_{15}4\Delta \end{bmatrix}$$

$$D_{ac} = \begin{bmatrix} a_{12} & a_{13} & a_{14} & a_{15} \\ c_{12} & c_{13} & c_{14} & c_{15} \\ a_{12}\Delta & a_{13}2\Delta & a_{14}3\Delta & a_{15}4\Delta \\ b_{12}\Delta & b_{13}2\Delta & b_{14}3\Delta & b_{15}4\Delta \end{bmatrix}$$

$$D_{ab} = \begin{bmatrix} a_{12} & a_{13} & a_{14} & a_{15} \\ b_{12} & b_{13} & b_{14} & b_{15} \\ a_{12}\Delta & a_{13}2\Delta & a_{14}3\Delta & a_{15}4\Delta \\ b_{12}\Delta & b_{13}2\Delta & b_{14}3\Delta & b_{15}4\Delta \end{bmatrix}$$

For conditions (B.1.11) through (B.1.13) to be true one has to examine the determinants individually. By properly partitioning one can derive the following:

$$|D_{bc}| = |D_{bc11}|\,|D_{bc22} - D_{bc21}D_{bc11}^{-1}D_{bc12}| \quad \text{if } D_{bc11}^{-1} \text{ exists.}$$

where it can be shown that

$$|D_{bc11}| = 4\cos\phi_2\cos\left(\frac{c_{12}+c_{22}}{2}\right)\sin\left(\frac{c_{12}-c_{22}}{2}\right)\cos\left(\frac{A_{13}+A_{23}}{2}\right)\sin\left(\frac{A_{13}-A_{23}}{2}\right)$$

$$- 4.\cos\phi_3\cos\left(\frac{c_{13}+c_{23}}{2}\right)\sin\left(\frac{c_{13}-c_{13}}{2}\right)\cos\left(\frac{C_{13}+C_{23}}{2}\right)\sin\left(\frac{C_{13}-C_{23}}{2}\right) \quad \text{(B.14)}$$

where ϕ_k , $C_1(\theta, t_k)$ and $C_2(\theta, t_k)$ are angles as defined in the Fig. B.1. The above two terms are identically zero iff:

i) $C_{12}+C_{22}=\pi$

ii) $C_{13}+C_{23}=\pi$

$\Rightarrow C_{1k}+C_{2k}=\pi$ (B.1.15)

i.e., motion along perpendicular bisector plane of the line joining the two sensors.

iii) $\phi_k = \frac{\pi}{2}$

iv) $A_{12}+A_{22}=\pi$

v) $A_{13}+A_{23}=\pi$

$\Rightarrow \phi_k=\frac{\pi}{2}$ and $A_{1k}+A_{2k}=\pi$ (B.1.16)

i.e., Target at infinite depth, a condition redundant for the problem defined as the depth is considered to be constant at z_0.

vi) $C_{12}=C_{22}$

vii) $C_{13}=C_{23}$

$\Rightarrow C_{1k}=C_{2k}$ (B.1.17)

i.e., Target at endfire or far-field.

viii) $A_{12}=A_{22}$

ix) $A_{13}=A_{23}$

$\Rightarrow A_{1k}=A_{2k}$ (B.1.18)

i.e., Target motion along perpendicular bisector plane of the line joining the two sensors or target at endfire or target at far-field. Finally, with some mathematical manipulations one can derive the following:

$$|D_{bc}| = \Delta^2\{12(b_{12}c_{13}-b_{13}c_{12})(a_{14}b_{15}-a_{15}b_{14})-4(b_{14}c_{13}-b_{13}c_{14})(a_{12}b_{15}-a_{15}b_{12})$$

$$-8(b_{12}c_{14}-b_{14}c_{12})(a_{13}b_{15}-a_{15}b_{13})-3(b_{14}c_{13}-b_{13}c_{14})(a_{14}b_{12}-a_{12}b_{14})$$

$$-6(b_{12}c_{15}-b_{15}c_{12})(a_{14}b_{13}-a_{13}b_{14})+2(a_{12}b_{13}-a_{13}b_{12})(b_{14}c_{15}-b_{15}c_{14})\} \quad \text{(B.1.19)}$$

Similarly,

$|D_{ac}| = |D_{ac11}||D_{ac22}-D_{ac21}D_{ac11}^{-1}D_{ac12}|$ if D_{ac11}^{-1} exists.

Also,

$$|D_{ac11}| = -4\sin(\frac{C_{12}+C_{22}}{2})\sin(\frac{C_{12}-C_{22}}{2})\cos(\frac{A_{13}+A_{23}}{2})\sin(\frac{A_{13}-A_{23}}{2})$$

$$+4\cos(\frac{A_{12}+A_{22}}{2})\sin(\frac{A_{12}-A_{22}}{2})\sin(\frac{C_{13}+C_{23}}{2})\sin(\frac{C_{13}-C_{23}}{2})$$

The above two terms in the R.H.S. are identically zero iff

i) $C_{12}=C_{23}$

ii) $C_{13}=C_{23}$

$\Rightarrow C_{1k}=C_{2k}$ (B.1.20)

i.e., Target located at enfire or far-field.

iii) $A_{13}=A_{23}$

iv) $A_{12}=A_{22}$

$$\Rightarrow A_{1k}=A_{2k} \tag{B.1.21}$$

i.e., Target motion along perpendicular bisector plane of the line joining the two sensors, or target located at endfire or far-field.

v) $A_{13}+A_{23}=\pi$

vi) $A_{12}+A_{22}=\pi$

$$\Rightarrow A_{1k}+A_{2k}=\pi \tag{B.1.22}$$

i.e., target at infinite depth, a condition ruled out for this problem.

As before one can derive the following expression:

$$\begin{aligned}|D_{ac}| = \Delta^2\{&12(a_{12}c_{13}-a_{13}c_{12})(a_{14}b_{15}-a_{15}b_{14})-4(a_{14}c_{13}-a_{13}c_{14})(a_{12}b_{15}-a_{15}b_{12})\\ &-8(a_{12}c_{14}-a_{14}c_{12})(a_{13}b_{15}-a_{15}b_{13})-3(a_{15}c_{13}-a_{13}c_{15})(a_{14}b_{12}-a_{12}b_{14})\\ &-6(a_{15}c_{12}-a_{12}c_{15})(a_{14}b_{13}-a_{13}b_{14})+2(a_{12}b_{13}-a_{13}b_{12})(a_{14}c_{15}-a_{15}c_{14})\}\end{aligned} \tag{B.1.23}$$

Similarly,

$$|D_{ab}| = |D_{ab11}|\,|D_{ab22}-D_{ab21}D_{ab11}^{-1}D_{ab12}| \quad \text{if } D_{ab11}^{-1} \text{ exists}$$

where,

$$\begin{aligned}|D_{ab11}| = &-4\cos\phi_3\sin\left(\frac{C_{12}+C_{22}}{2}\right)\sin\left(\frac{C_{12}-C_{22}}{2}\right)\cos\left(\frac{C_{13}+C_{23}}{2}\right)\sin\left(\frac{C_{13}-C_{23}}{2}\right)\\ &+4\cos\phi_2\cos\left(\frac{C_{12}-C_{22}}{2}\right)\sin\left(\frac{C_{12}-C_{22}}{2}\right)\sin\left(\frac{C_{13}+C_{23}}{2}\right)\sin\left(\frac{C_{13}-C_{23}}{2}\right)\end{aligned} \tag{B.1.24}$$

The last two terms are identically zero if,

i) $C_{12}+C_{22}=\pi$

ii) $C_{13}+C_{23}=\pi$

$\Rightarrow C_{1k}+C_{2k}=\pi$ (B.1.25)

i.e., Target motion along perpendicular bisector plane of the line joining the two sensors.

iii) $C_{12}=C_{22}$

iv) $C_{13}=C_{23}$

$\Rightarrow C_{1k}=C_{2k}$ (B.1.26)

i.e., Target located at endfire or far-field.

v) $\phi_k=\frac{\pi}{2}$ (B.1.27)

i.e., target at infinite depth, a condition ruled out for this problem.

As before one can show that

$$|D_{ab}| = \Delta^2\{12(a_{12}b_{13}-a_{13}b_{12})(a_{14}b_5-a_{15}b_{14})-4(a_{14}b_{13}-a_{13}b_{14})(a_{12}b_{15}-a_{15}b_{12})$$
$$-8(a_{12}b_{14}-a_{14}b_{12})(a_{13}b_{15}-a_{15}b_{13})-3(a_{15}b_{13}-a_{13}b_{15})(a_{14}b_{12}-a_{12}b_{14})$$
$$-6(a_{12}b_{15}-a_{15}b_{12})(a_{14}b_{13}-a_{13}b_{14})+2(a_{12}b_{13}-a_{13}b_{12})(a_{14}b_{15}-a_{15}b_{14})\} \quad \text{(B.1.28)}$$

One can now combine conditions (1) through (6) and the respective equations to determine the determinant of D_1

Sufficient Conditions of Unidentifiability

From the above analysis it is clear that for determinant of the main matrix D_1 to be zero the determinant of all 2x2 submatrices must be zero. The details of the workout can be obtained in [29]. Also on inspection all the above conditions reduce to the following three important conditions as follows:

i) $C_{1k}+C_{2k}=\pi$

$$\Rightarrow B_{1k}+B_{2k}=\pi \tag{B.1.29}$$

i.e., Target motion along perpendicular bisector plane of the line joining the two sensors.

ii) $C_{1k}=C_{2k}$

$$\Rightarrow B_{1k}=B_{2k} \tag{B.1.30}$$

i.e., Target *located at endfire or far-field.*

iii) $A_{1k}=A_{2k}$ (B.1.31)

i.e., Target located at endfire or far-field, or target motion along the perpendicular bisector plane of the line joining the two sensors.

B.2 *Step II-TDOA and depression angle measurements*

In this case one has to show that the |D| exists where:

$$|D| = \begin{vmatrix} A_1 & A_2 & A_3 & A_4 & A_5 \\ B_1 & B_2 & B_3 & B_4 & B_5 \\ C_1 & C_2 & C_3 & C_4 & C_5 \\ A_1t_1 & A_2t_2 & A_3t_3 & A_4t_4 & A_5t_5 \\ B_1t_1 & B_2t_2 & B_3t_3 & B_4t_4 & B_5t_5 \end{vmatrix} \tag{B.2.1}$$

From Ref. [14]-[16] it is sufficient to show that $|D_1| + |D_2| + |D_3|$ is non-zero, where D_1, D_2 and D_3 are as defined in Section II. Existence of the first term is already shown in Step I above. If one works through the evaluation of $|D_2|$ and $|D_3|$ one can show that:

$$|D_1| + |D_2| + |D_3|$$

$$= \Delta^2\{12H(K'-X'+T')-4S(L'-Y'+P')-8Q(N'-Z'+R')$$

$$+3R(M'-V'+Q')-6P(O'-V'+S')+2T(F'-G'+H')\} \qquad (B.3.2)$$

where the constants can be obtained from [29]. On closer examination of Eqn. (B.3.2) it is clear that the terms on the R.H.S. are identically zero if the submatrices of determinants D_1, D_2 and D_3 are zero which as in step one reduces to the three main conditions as in the Equations (B.29) (B.30) and (B.31).

B.3 Identifiability condition for the three-dimensional case when only frequency measurements are considered

When the FIM is evaluated by considering the single-sensor target frequency measurements obtained with two sensors, the target is generally identifiable. The sufficient conditions of unidentifiability are developed as follows: In this case one has to show that the determinant of the matrix D_i, i=4,5 is non-zero, where the $|D_i|$ is given by

$$|D_i| = \begin{vmatrix} a_{i1} & a_{i2} & a_{i3} & a_{i4} & a_{i5} \\ b_{i1} & b_{i2} & b_{i3} & b_{i4} & b_{i5} \\ c_{i1} & c_{i2} & c_{i3} & c_{i4} & c_{i5} \\ d_{i1} & d_{i2} & d_{i3} & d_{i4} & d_{i5} \\ e_{i1} & e_{i2} & e_{i3} & e_{i4} & e_{i5} \end{vmatrix} \quad i=4,5 \qquad (B.3.1)$$

where the quantities that make up the determinant are obtained from Appendix A. As before, one can develop the determinant along the first column giving the sufficient conditions for the $|D_i|$ to be zero. The basic conditions are

1) a_{ik}=0, or its minor=0 and, (B.3.2)

2) b_{ik}=0 or its minor=0 and, (B.3.3)

3) c_{ik}=0 or its minor=0 and, (B.3.4)

4) d_{ik}=0 or its minor=0 and, (B.3.5)

5) e_{ik}=0 or its minor=0 and, (B.3.6)

where i=4,5 and k=1,...5, (since the minimum number of measurements are considered.)

When the target is at endfire and moving along the line joining the two sensors, then v_x is some value say 10 kn and v_y=0, one can show from the Eq. (B.3.2) that

$$1=(\cos B_{ik}\cos A_{ik})^2 \quad (B.3.7)$$

which is true, since A_{ik} and B_{ik} are both zero.

Similarly, one can show that the Eq. (B.3.3) reduces to

$$\cos B_{ik}\cos A_{ik}\sin B_{ik}\cos A_{ik}=0 \quad (B.3.8)$$

which is true, since A_{ik} and B_{ik} are both zero.

Similarly, under the above conditions the Eq. (B.3.4) reduces to

$$\tan A_{ik}\cos B_{ik}\cos A_{ik}=0 \quad (B.3.9)$$

which is true, since A_{ik} and B_{ik} are both zero. The minors of d_{ik} and e_{ik} eventually reduce to zero as a consequence of the Equations (B.3.7), (B.3.8) and (B.3.9).

When the target is at far-field it can be considered moving perpendicular to the line joining the two sensors which means v_x=0 and v_y is some value say 10 kn, then the Eq. (B.3.2) reduces to

$$\sin B_{ik}\cos A_{ik}\cos B_{ik}\cos A_{ik}=0 \quad (B.3.10)$$

which is true since $B_{ik}=90^o$ and A_{ik}=0.

Similarly, Eq. (B.3.3) reduces to

$$(\sin B_{ik}\cos A_{ik})^2=1 \qquad (B.3.11)$$

which is true since $B_{ik}=90^o$ and $A_{ik}=0$.

Also Eq. (B.3.4) reduces to

$$\tan A_{ik}\sin B_{ik}\cos A_{ik}=0 \qquad (B.3.12)$$

which is also true since $A_{ik}=0$, as before the minors of d_{ik} and e_{ik} eventually reduce to zero as a consequence of the Equations (B.3.10), (B.3.11), and (B.3.12). Thus target unidentifiable if at endfire or far-field.

When the target is moving along the perpendicular bisector plane of the line joining the two sensors it is convenient to consider the convenient to consider the complete FIM and then evaluate the determinant of the combined FIM. In this case the target still moves perpendicular to the line joining the two sensors so that $v_x=0$ and v_y is some value say 10 kn, in which case a_{4k} & $a_{5k} \neq 0$ and b_{4k} & $b_{5k} \neq 0$, since $B_{1k} + B_{2k} = 180^o$, and thus for motion along the perpendicular bisector plane of the line joining the two sensors the target is identifiable.

REFERENCES

[1] R.O. Schmidt, " A new approach to geometry of range difference location, " IEEE Trans. Aerosp. Electron. Syst. vol. AES-8, pp.821-835, Nov. 1972.

[2] E. Weinstein, " Optimal source localization and tracking from passive array measurements," IEEE Trans. Acoust., Speech, Signal Processing, vol. ASSP-30, no. 1, pp. 69-76, Feb. 1982.

[3] V. H. MacDonald and P. M. Schultheiss, " Optimum passive bearing estimation in a spatially incoherent noise environment, " J. Acoust. Soc. Amer., vol. 46, no. 1, pp.37-43, 1969.

[4] W. R. Hahn, " Optimum signal processing for passive sonar range and bearing estimation, "J. Acoust. Soc. Amer., vol. 58, no. 1, pp. 201-207, July 1975.

[5] E. J. Hilliard and R. F. Pinkos, " Analysis of triangular ranging using beta density angular errors, " J. Acoust. Soc. Amer.," vol. 65, no. 5, pp. 1218-1228, May 1979.

[6] G. C. Carter, " Variance bounds for passively locating an acoustic source with a symmetric line array, " J. Acost. Soc. Amer., vol. 62, pp. 922-926, Oct. 1977.

[7] J. F. Arnold, Y. Bar-Shalom, R. Estrada, R. A. Mucci, " Target parameter estimation using measurements acquired with a small number of sensors. " IEEE J. Oceanic Engg. vol. OE-8, no.3, July 1983.

[8] J. M. Fitts, " On the observability of nonlinear systems with applications to nonlinear regression analysis, " in Proc. Symp. Non-linear Estimation Theory and its Application (San Diego, CA), Sept. 1970.

[9] H. Cramer, Mathematical Methods of Statistics. Princeton, NJ: Princeton University Press, 1951.

[10] H. L. Van Trees, Detection, Estimation, and Modulation Theory-Part I Detection, Estimation, and Linear Modulation Theory. New York: Wiley, 1968.

[11] W. R. Hahn and S. A. Tretter, " Optimum processing for delay vector estimation in passive sonar arrays, " IEEE Trans. Inform. Theory, vol.IT-19, no. 5, pp. 608-614, Sept. 1973.

[12] P. M. Schultheiss and E. Weinstein, " Lower bounds on the localization errors of a moving source observed by a passive array, "

IEEE Trans. Acoust. Speech, Signal Processing, vol. ASSP-29, no. 3, pp. 600-607, June 1981.

[13] C. H. Knapp and G. C. Carter, " The generalized correlation method for estimation of time delay, " IEEE Trans. Acoust., Speech, Signal Processing, vol. ASSP-24, no. 4, pp. 320-327, Aug. 1976.

[14] T. Fujisawa and E. S. Kuh, " Some results on existence and uniqueness of solutions of nonlinear networks, " IEEE Trans. Circuit Theory, vol. CT-18, pp. 501-506, Sept.1971.

[15] S. R. Kuo, D. L. Eliott, T. J. Tarn, " Observability of nonlinear systems, " Inform. Contr., vol. 22, pp. 89-99, 1973.

[16] T. Ohtsuki and H. Watanabe, " State-variable analysis of RLC networks containing nonlinear coupling devices, " IEEE Trans. Circuit Theory, vol. CT-16, pp. 26-38, Feb. 1969.

[17] E. Weinstein, " Measurement of the differential doppler shift, " IEEE Trans. Acoust., Speech, Signal Processing, vol. ASSP-30, no. 1, pp. 112-117, Feb. 1982.

[18] P. M. Schultheiss and E. Weinstein, " Estimation of differential doppler shifts, " J. Acoust. Soc. Amer. vol. 66, pp. 1412, Nov. 1979.

[19] M. J. Shensa, " On the uniqueness of doppler tracking, " J. Acoust. Soc. Amer., vol. 70, no. 4, pp. 1062-1064, Oct. 1981.

[20] S. Nardone and V. Aidala, " Observability criteria for bearing-only target motion analysis, " IEEE Trans. Aerosp. Electron. Syst., vol. AES-17, pp. 162-166, Mar. 1981.

[21] J. H. Wilkinson, The Algebraic Eigen Value Problem Oxford, England: Clarendon Press, 1965.

[22] R. A. Altes, " Target position estimation in radar and sonar, and generalized ambiguity analysis for maximum likelihood parameter estimation, " Proc. IEEE, vol. 67, no. 6, pp. 920-930, June 1979.

[23] R. Fletcher and M. J. D. Powell, " A rapidly convergent descent method for minimization, " Comput. J., vol. 6, no. 2, pp. 163-168, 1963.

[24] E. Weinstein, " Decentralization of the Gausian maximum likelihood estimator and its applications to passive array processing, " IEEE Trans. Acoust. Speech, Signal Processing vol. ASSP-29, no. 5, pp. 945-951, Oct. 1981.

[25] R. R. Tenney and N. R. Sandell, Jr., " Detection with distributed sensors, " IEEE Trans. Aerosp. Electron. Syst., vol. AES-17, no. 4, pp. 501-507, July 1981.

[26] V. R. Lessor and L. D. Erman, " Distributed interpretation: A model and experiment, " IEEE Trans. Comput., vol. C-29, no. 12, pp. 1144-1162, Dec.1980.

[27] J. Arnold, Y. Bar-Shalom, and R. Mucci, " Track Segment Association with a Distributed Field of Sensors, " Proc. American Control Conference, San Diego, CA, June 1984.

[28] D. G. Luenberger, " Introduction to Linear and Non- Linear Programming " Addison-Wesley, 1973.

[29] H. M. Shertukde, " Target parameter estimation with a single pair of sensors using Time difference of aarival and depression angle measurements", M. S. Thesis, University of Connecticut, EECS, Dec. 1985.

END

FILMED

4-85

DTIC